

Manuscript ESSD-2017-119 – Responses to reviewers

We thank the reviewers and the associate editor for their thorough reading of the manuscript and for their constructive criticisms. We have modified the paper following their suggestions and we believe that the manuscript has improved thanks to them.

Our responses are detailed in the following, addressing all the points raised by the reviewers. The responses hereinafter and the corresponding changes in the revised manuscript appear in blue for convenience.

Associate editor:

The paper lacks important information on the existing knowledge on (i) biochemistry in the Mediterranean and changes (ii) historical data and gaps in observing systems. Such information should partially justify the important efforts done during the Tethys cruise.

The BGC-Argo program has been developed in the context of stock assessments of phytoplankton biomass over oceanic basins, and the underlying changes at seasonal scales and under increasing anthropic perturbations. We believe that these aspects have been described in the Section 1.1, with an overview of the biogeochemistry in the Mediterranean (the typical functioning, the large-scale gradients, the different trophic regimes distributed as bio-provinces). As also suggested by the reviewer #1, the dataset is now presented in the context of this existing knowledge, see Section 4 in the revised manuscript.

Concerning observing systems, the Section 1.1 provides elements of historical archives (mainly ocean color products, time-series at observation sites as Dyfamed); it is stressed how the gaps of this observing system (mainly the vertical structuration of biomass at seasonal scales) can be filled by BGC-Argo data.

There is another aspect that should be included in the paper: are there seasonal changes? Can a single cruise provide useful information to assess seasonal variabilities?

Seasonal changes on biogeochemistry in the Mediterranean Sea have been studied from satellite ocean color records as mentioned in Section 1.1. Different trophic regimes have been characterized from seasonal cycles of surface chlorophyll-a concentration. This bio-regionalization revealed that a single cruise can provide useful information on spatial distributions (bioregions) but would need more intensive surveys to catch the seasonal signals. This is the motivation of this association of a cruise for reference data and time extension from BGC-Argo floats. These elements appear in the Section 4 of the revised manuscript.

The paper is going to much in details on qc procedures, that can be found in other publications and reports and is not providing any information on the contribution to the scientific knowledge on the Mediterranean ecosystems.

This comment has also been pointed out by the two reviewers and a major revision of the manuscript has been made to reduce information on qc procedures. Changes are detailed hereinafter in the responses to the reviewers' comments.

Reviewer #1:

Data format is understandable, adequate for a spreadsheet thought not following standards as e.g. SeaDataNet nor using a Hierarchical Data Format to ease the direct access from users. This forces the user to implement its own code to import the dataset into analysis software.

The data format consists in tables constructed as comma separated values, archived in Ascii files, with a full description of the data collection. This choice has been suggested by the data manager that attributed the doi number to this dataset, in order not to restrict to any specific analysis software. This data format has not been modified, also following the appreciation of the reviewer #2.

My main concern about the paper is that there is an extensive description of data collection and processing procedures (too detailed in my view), while the presentation of the record is almost absent.

We have followed the recommendation of the reviewer: in the revised manuscript, the description of the processing procedures and qc protocols have been simplified (important cuts in the text of Section 2 and four tables suppressed) whereas the presentation of the record has been developed (two new figures and a new paragraph in Section 4). Details on the underlying modifications are drawn hereinafter.

I would suggest the authors to reduce the details on processing whenever it follows any published protocol, and also reduce the details of calibration coefficients/parameters determination.

Major changes have been achieved in the Section 2 in order to simplify the description of the sensing methods and QC protocols. Here is a detailed list of the changes achieved in the revised manuscript.

Section 2.2.1: details on deployment procedure of deployment for CTD underwater unit have been removed as it followed the standard procedure of the GO-SHIP manual.

Section 2.2.2: details on data processing for TSG and CTD profiles have been removed (and references therein) as they followed the standard procedure of the GO-SHIP manual.

Section 2.3.1: details on the Winkler method have been removed as they followed the recommendations of Langdon (2010). The description of the functioning for the electrochemical sensor as well as the optode sensors (and references therein) has been simplified.

Section 2.3.2: details on the Winkler protocol have been removed as they followed the recommendations of Langdon (2010).

Section 2.4.2: details on the linear regression model (and references therein) have been removed. Description of data processing for TSG fluorescence has been simplified.

Section 2.4.3: The quality control of HPLC data has been simplified as it followed the recommendations of Ras et al. (2008).

Section 2.5.1: details on nutrient sampling and titration (and reference therein) have been removed as they followed the recommendations of Kirkwood (1992) and Aminot and Kerouel (2007). Details on nitrate optical sensing (and references therein) have been removed.

Section 2.5.2: details on the data processing algorithm have been removed as they are reported in Paqueron et al. (2015).

The revised draft should substantially reduce the details on processing and avoid most tables (up to 8 in the current version) ...

Following the reviewer's recommendation, four tables have been removed in the revised manuscript.

Section 2.1.3: the Table 4 has been suppressed accordingly and a sentence reporting the assessment has been added.

Section 2.2.3: the Table 5 has been removed and only the regression coefficient have been reported in the text.

Section 2.3.2: the Tables 6 and 7 have been removed as the description of the processing procedure has been simplified.

Section 2.4.2: the Figure 3 has been removed as it provided redundant information with the text. The Table 8 has been renamed as Table 4.

... and include figures of the measured fields (CTD profiles, LADCP profiles, biogeochemical) so readers can see spatial changes across different basins. SADCP record should also be shown as an

oceanographic section.

A new paragraph has been added at the beginning of the Section 4 of the revised manuscript. The record is presented in the frame of existing knowledge of the Mediterranean hydrology and biogeochemistry, in order to introduce the complementarity between the cruise and BGC-Argo. As suggested by the reviewer, two figures have been added for this purpose: a SADCP section in Figure 3, TS diagrams from CTD casts in Figure 4 (upper left panel), oxygen concentration profiles from CTD casts in Figure 4 (lower left panel), total chlorophyll-a concentration and nitrate concentration from water samples in Figure 4 (right panels).

I also miss extended discussion on the role of short-term variability in the misfit between CTD profiles and Argo floats (e.g. is the misfit in Argo vs CTD hydrography comparable for example to that seen among consecutive CTDs at the same site?).

The reviewer is right to underline that short-term variability can affect the comparison between CTD and BGC-Argo profiles, introducing natural variability in the measured misfit. This point will be discussed hereinafter in the response of a specific comment in the case of hydrology and on the mesoscale effects. The issue is even more challenging for some biogeochemical variables, that have signal on surface affected by diurnal cycle. We believe that a perfect concomitancy (float clamped in the CTD-Carousel) is the only way to characterize possible calibration shifts at deployment, but our ancillary dataset is still too small to provide a quantitative answer to this point. A sentence has been added in Section 4 to mention the reviewer's comment in the revised manuscript.

Finally, it would be interesting to see (graphically) how nutrients and O₂ at depth relate to known background climatological fields.

The suggestion of the reviewer is fair, as soon as our report provides verification and quality control of the records by the comparison of several in-situ sensing methods rather than comparing them to climatology. Following the reviewer's comment, the dataset of oxygen and nitrate concentration has been replaced among previous large-scale field surveys (BOUM in 2009 and M83/4 in 2011). A sentence has been added in Section 4, first paragraph, of the revised manuscript.

p2. 1.4-5. Provide references on these “few ocean observation sites”.

Done

Section 1.2. I understand that the cruise is dedicated to the maintenance of the Argo- BGC fleet by adding more floats to the array. Some questions arise to me: Can you provide info on how many buoys were active at the time of the cruise?

At the time of the cruise there were 12 active BGC-Argo floats. This information has been added in the revised manuscript.

Was not possible to perform any calibration profile at positions of active Argo-BGC at the time of the cruise?

Among the active floats, 4 have been recovered and renewed during the cruise. This allowed to provide a post-mission calibration for these floats. The other active floats could not be reached given the available ship time and the constraints of regular port calls; their mission finished within the year without recovery.

Where were the 10 floats deployed? I assume 7 were launched at the CTD positions provided but what about the remaining three? Do these correspond to the Levantine basin?

The position of the 9 floats concerned by calibration exercises has been added in the Table 2. As explained in Section 1.2, we have encountered problems for working clearance in the Levantine basin.

Thus one float has been deployed without CTD cast (it does not appear in Table 2), and two other floats have been deployed in another location after calibration exercise at a CTD station (they appear in Table 2 with a star).

p3. 1.20. Why only the LOV BGC-Argo were considered?

This sentence has been rewritten in the revised manuscript: we were meaning that only BGC-Argo floats were considered as several physical Argo floats have been also deployed during the cruise.

p3. 1.26. “Note that the floats were programmed to profile everyday at noon”. Should be pointed before, readers not familiar with this array expect Argo floats to profile once every 10 days. Moreover you have said that the floats cycle on weekly basis (p.2 1.8) and again say in the conclusions.

The cycling rate can be changed during missions thanks to Iridium communications (detailed in Leymarie et al., 2013). The current cycling period is on a weekly basis; however a daily cycling has used at the beginning of the mission in order to increase concomitancy with the CTD cast. This point has been clarified in the revised manuscript.

p3. para6. Please explain better, didn't you get permission to perform CTDs in the Levantine basin but to sail there and launch Argo floats?

We have got working clearance from the Greek authorities to perform CTD casts in the Levantine basin. However, a Turkish warship surveying this area during our cruise did not allow us to perform these CTD casts.

Section 2.1.2. The reference Le Bot et. al. is absent in the bibliography. Could you explain differences (if any) between the Cascade processing and the more widespread software CODAS?

CASCADE is the software used in routine to process VM-ADCP data collected in the French RV fleet. The principles of the two softwares are the same: edit and correct doubtful profiles, integrate navigation data in the processing. As underlined by the reviewer #2, CODAS proposes more options for the calibration aspects of the ADCP, in particular the calculation of misalignment angle of the instrument that would have prevented the L-shape calibration exercise performed during the cruise. A sentence has been added in section 2.1.3 and the reference of Le Bot et al. has been added to the revised manuscript.

Could you comment further in the bottom track correction through Gebco?

The reviewer is right to ask for clarification: actually no correction has been performed, only a mask on bottom detections using Gebco has been applied. The manuscript has been revised in agreement.

It is not clear to me whether you use LADCP downlooker bottom track to constrain the final profile solution.

The information if whether the bottom track is used or not in the final computation only appears in Table 3. For sake of reducing the processing details, the manuscript has not been modified according to this point.

p7. 1.22– explain further why choosing the layer 750–1000 m, how does the de- correlation scale increase with depth? Is 750 m deeper than the extent of a typical eddy?

This is a difficult point to determine whether natural variability or instrumental shift cause misfits between CTD and float profiles. The main motivation of choosing the layer 750-1000 m is to compare characteristics of stable water masses (under the LIW) that should be less influenced by short scale variability of surface layer dynamics. The last paragraph of Section 2.2.3 has been rewritten according to the reviewer's comment in the revised manuscript.

Considering mesoscale variability (that can extend under 750 m), the distance between CTD and float

profiles remain short (few kilometers) with respect to the size of typical eddies (60 km). Moreover, the duration between profiles (less than 2 days) should remain short enough with respect to the displacement of typical eddies (some kilometers per day) to consider that the two profiles would keep influenced equally by mesoscale effects. A sentence has been added in Section 4 to mention the reviewer's comment.

1.25, what is the 0.01°C (or in PS) threshold?

The accuracy of 0.01 referred to Argo standards for uncertainties of measurements. This notion of threshold, unclear in this context, has been removed in the revised manuscript.

p9. 1.15 Regarding the O2 sensor hysteresis correction, are you following any Sbe technical note directly (if so please indicate which version) or did you programmed specific software?

The SBE technical note (AN64-2) has been followed directly to modify the algorithm of Owens and Millard (1985). The reference has been added in the revised manuscript.

1.21 why 2.8 standard deviation?

The outliers are classically edited by comparing individual misfits to the overall standard deviation, that requires the specification of a threshold value. In our processing the threshold value of 2.8 standard deviation was set to edit outliers.

1.25 Why do you use CTD temp instead of the built-in temperature of Rinko software? You cannot account for inner sensor thermal lag using an external thermometer.

Considering optodes, built-in temperature is measured by an external sensor as there is no plumbing inside the sensor. We believe that the temperature at the location of the foil, used to derive dissolved oxygen concentrations by the Rinko software, would be the seawater temperature as effects of thermal cell inertia should not be significant compared to the accuracy and dynamical responses of built-in temperature sensors.

p.15 l. 24– I do think that a Dataset including pre and post mission calibration would be very valuable.

We agree with the reviewer: the records of this cruise provide valuable ancillary data for the BGC-Argo missions. They are archived to perform and distribute to the users community delayed mode adjustments in the time series of the BGC-Argo floats. A sentence has been added in Section 4 of the revised manuscript.

p.22 (Table 2). Provide deployment positions.

The Table 2 has been modified following the reviewer's comment. Only WMO number has been kept and a column with station deployment has been added.

p.23 (Table 3). How is the error magnitude compared to the actual velocity?

We are not sure to understand this comment. LADCP data processing with the software LDEO provides horizontal velocity profiles together with associated uncertainties (error velocity magnitude) by minimizing the misfits to different constraints.

p.28 (Fig.2). Should not the residuals of the Rinko sensor provide zero-average bias after the calibration against Winkler?

The Figure 2 shows the residuals between the Rinko sensor and Winkler measurements, before calibration against Winkler. A pressure-dependent slope is reported in Section 2.3.3, however a post-cruise processing of the Rinko data cannot be achieved because the calibration coefficients of this sensor are not available. That is why the SBE43 data have been used rather than Rinko data in the final dataset. This is now clearly mentioned in the revised manuscript.

p2. 1.30 “are to be” sounds weird to me. Next sentence delete “and”.

Done

p3. 1.2. 3000nm, add space. Also along para.3 (1000m etc)

Done

p3. 1.25. Re-word “calibration exercises could have been drawn”.

Done

p4. 1.26 I would say assembled instead composed.

Done

p8. 1.1. The date in ref to Winkler work does not match that on the bibliographic list.

Done

p12. 1.31 should read right panel.

Done

p15. 1.20 replace “until” by “up to”

Done

Reviewer #2:

The description of observation methods and data processing is clear and detailed (maybe sometimes even too detailed for those observation methods which are standard procedures).

The descriptions of standard procedures for sensing, processing and quality control have been reduced in the revised manuscript.

The data and presentation quality is good and the data is accessible under the corresponding doi number.

We followed the appreciation of the reviewer: the format for the archive of the dataset has not been modified.

Title: could be improved. For example: Hydrography and biogeochemics in the Mediterranean Sea during a cruise with RV Tethys 2 in May 2015 to calibrate BGC-Argo floats

We followed the suggestion of the reviewer.

Page 1, line 25: for (instead of to) temperature ...?

We did not find this typo.

Page 3, line 8-13: this is standard for a research vessel, can be shortened.

This paragraph has been cut in the revised version and main information moved to the following paragraph.

Page 3, line 15-16: I understand that usually two casts were taken at a station. But what about samples? Were they taken at standard depths? Or, different depths at different stations?

The deep cast was composed of only standard levels, whereas the sampling around the deep chlorophyll maximum was refined during the shallow cast. The sampling strategy is now detailed in the revised manuscript.

Page 5, line 4: When CTD profile available ... were available

Done

Page 5, line 8-14: I am not sure if I got it right: the transects had to be done in order to correct the misalignment angle of the ADCP? If so, you should use i.e. the CODAS software (Hawaii) for ADCP data analysis, this calculation is included there.

The reviewer is right: contrary to CASCADE software, CODAS software proposes the option to correct the misalignment angle of the ADCP, that would have prevented the L-shape calibration exercise performed during the cruise. A sentence has been added in section 2.1.3 of the revised manuscript.

Page 7, paragraph 2.2.3: just a comment: it is uncommon, not to check especially salinity against samples, also in case of the TSG. You were lucky that your sensors remained stable. In case not, you would not be able to reproduce the station when it happened and to correct values accordingly.

Thank you for this comment. This comparison takes less space in the revised manuscript while the Table 5 have been cut.

Page 8, line 1: I guess it is 1988 instead of 1888.

Even if we understand that it could appear to be strange, it is interesting to note that the original paper of the Winkler method has been published in 1888 and that this method has remained the standard method to this day with only marginal improvements that are taken into account in the recommendations of Langdon 2010. However, as mentioned by reviewer 1, in the reference list the publication of Winkler was incorrectly reported with the year 1988.

Page 8, 1-30: to my opinion too detailed, it is standard method

The Section 2.3.1 has been simplified and strongly reduced in the revised manuscript (see response to reviewer #1 for details).

Page 12, line 23 instead of upper panel, left panel?

The Figure 3 has been suppressed following the suggestion of the reviewer #1.

Table 3 is confusing: in LDEO you list the components but in the following columns you calculate it with and without these components? It's a contradiction?

For every casts, the error velocities were computed for three sets of profiles: one as measured by LADCP only, one as measured as SADCP only, and one as processed from LADCP measurements under SADCP constraint. In function of the results were chosen the final process parameters reported in the column. The order of the columns of the table and the table caption have been changed in the revised manuscript.

Hydrography and biogeochemistry dedicated to the Mediterranean BGC-Argo network during a cruise with RV Tethys 2 in May 2015

Vincent Taillandier¹, Thibaut Wagener², Fabrizio D'Ortenzio¹, Nicolas Mayot^{1,+}, Hervé Legoff³,
Joséphine Ras¹, Laurent Coppola¹, Orens Pasqueron de Fommervault^{1,*}, Catherine Schmechtig⁴, Emilie
5 Diamond¹, Henry Bittig¹, Dominique Lefevre², Edouard Leymarie¹, Antoine Poteau¹, Louis Prieur¹

¹Sorbonne Universités, UPMC Université Paris 06, CNRS, LOV, Villefranche-sur-Mer, 06230, France

²Aix-Marseille Université, CNRS/INSU, Université de Toulon, IRD, Mediterranean Institute of Oceanography (MIO), UM
110, Marseille, 13288, France

³Sorbonne Universités, UPMC Univ Paris 06, CNRS, IRD, MNHN, LOCEAN, Paris, France

10 ⁴Sorbonne Universités, UPMC Univ Paris 06, CNRS, UMS 3455, OSU Ecce-Terra, Paris Cedex 5, France

⁺ present affiliation: Bigelow Laboratory for Ocean Sciences, Maine, USA

^{*} present affiliation: Laboratorio de Oceanografía Física, CICESE, Ensenada, B.C., Mexico

Correspondence to: Vincent Taillandier (taillandier@obs-vlfr.fr)

Abstract

15 We report on data from an oceanographic cruise, covering western, central and eastern parts of the Mediterranean Sea, on the
French research vessel Tethys 2 in May 2015. This cruise was fully dedicated to the maintenance and the metrological
verification of a biogeochemical observing system based on a fleet of BGC-Argo floats. During the cruise, a comprehensive
dataset of parameters sensed by the autonomous network was collected. The measurements include ocean currents, seawater
salinity and temperature, concentration of inorganic nutrients, of dissolved oxygen, and chlorophyll pigments. The analytical
20 protocols and data processing methods are detailed, together with a first assessment of the calibration state for all the sensors
deployed during the cruise. Data collected at stations are available under doi:10.17882/51678, data collected along ship track
are available under doi:10.17882/51691.

1 Introduction

1.1 Context of the cruise

25 The biogeochemical functioning of the Mediterranean Sea is typical of temperate oceanic regions. Seasonal dynamics of
phytoplankton follow an increase of biomass in spring even if primary production remains low during the whole year (Marty
et al., 2002). The biomass distribution in the Mediterranean Sea is marked by a pronounced east-west gradient (Bosc et al.,
2004). This pattern is confirmed by the phenology of the underlying phytoplankton dynamics, that vary from ultra-oligotrophic
regimes in the oriental basin to bloom regimes in the north-western basin (D'Ortenzio et al., 2009). An extended study on the
30 geographical distribution of these regimes – related to the Mediterranean bio-provinces – has revealed significant changes at
regional scales during the last decades (Mayot et al., 2016). Indeed, the seasonal cycle of biomass concentration turns out to
be a reliable indicator of the response of pelagic ecosystems to external perturbations (Siokou-Frangou et al., 2010). Under

increasing anthropic effects and considered as regional hotspot where impacts of climate change will be the largest (Giorgi and Lionello, 2008), the Mediterranean Sea appears to be a key-basin to characterize this indicator under a large panel of possible trophic regimes as well as various physical and chemical environments (Durrieu de Madron et al., 2011).

5 The seasonal cycles of biomass concentration have mainly been observed from satellite images of ocean colour, thanks to their synoptic coverage of the area. However limited to surface characterization, the link between biomass structuration in the water column and the underlying physical-chemical state over a seasonal scale has only been achieved in few ocean observation sites (Marty and Chiaverini, 2010). The emergence of BGC-Argo floats, which are autonomous profiling platforms embarking biogeochemical sensors and programmed to weekly cycle until 1000-meter depth (Leymarie et al., 2013), now allows to collect oceanographic profiles concomitantly for physical and biogeochemical properties (temperature, salinity, concentration of dissolved oxygen, chlorophyll-a, nitrate). These open new perspectives for the description and comprehension of the biogeochemical functioning of the Mediterranean Sea. For example, the occurrence of phytoplankton blooms can be directly related to the availability of nutrients (D'Ortenzio et al., 2014).

15 Such technological advances encouraged to set up a dedicated observing system over the Mediterranean Sea with a fleet of a dozen of BGC-Argo floats in operation. This emerging network has been promoted and sustained by French programs such as Equipex-NAOS and the Mermex experiment, as well as at the European level through Euro-Argo infrastructure. However, sensors for biogeochemical properties, even with recent factory calibration, are subject to substantial systematic errors when deployed on BGC-Argo floats, as reported by Bittig et al. (2012) for oxygen measurements or by Pasqueron de Fommervault et al. (2015) for nitrate measurements. In consequence, even if a BGC-Argo float is supposed to be completely autonomous after deployment, reference data for quality assessment of most of its sensors needs to be collected from ship (D'Ortenzio et al., 2014; Johnson et al., 2017). Automatic quality controls are rapidly advancing at the Argo instances (Schmechtig et al., 2015), although most of the methods and protocols are still under assessment. In this context, a dedicated and accurate effort was mandatory to ensure the quality of the data of the Mediterranean observing system composed of BGC-Argo floats.

1.2 Objectives and achievements of the cruise

25 The dataset presented in this paper was collected during an oceanographic cruise carried out in Spring 2015 over the Mediterranean Sea. In our knowledge, it was the first cruise fully dedicated to the maintenance and the metrological verification of an autonomous observing system based on BGC-Argo floats. The objectives of the cruise were twice:

- continue the time series of profile collection that have been set up since 2012 over the Mediterranean Sea, by deploying new BGC-Argo floats and recovering old ones,
- perform the harmonisation of the collection, with a systematic verification of the calibration state for all the biogeochemical sensors that have been active in the network, using shipboard measurements as standards of reference.

30 The choice of a dedicated cruise instead of ships of opportunity was motivated by applying the same protocol of metrological verification for all the floats, using the same instruments and methods of reference. Another crucial point remains on the required flexibility to choose the location of the oceanographic stations, which mainly depended on the state of the network (i.e. the position of the different floats) at the time of the cruise.

The survey covered large parts of the western, central and eastern basins of the Mediterranean Sea with a total route of about 3000 nm (Figure 1). The cruise started in Nice (France) on May 12th 2015 and ended up in Nice on June 1st 2015, on board the Tethys 2 which is a 24-meter-long research vessel of the French research national institute (CNRS). The crew was composed of seven mariners and five scientists. The cruise was divided in four legs of about four days: three port calls were programmed on 18-19 May in Heraklion (Crete, Greece), on 24-25 May in Heraklion, and on 28-29 May in Lipari (Sicily, Italy). The initial cruise planning ended up to be composed of seven oceanographic stations, which represents about two stations of 10 hours per leg. Transects between stations were crossed at 8-11 knots depending on sea conditions.

Work on board during the transects was dedicated to the surface sampling, together with seawater sample analyses and data processing. During stations, a CTD-Carousel composed of 11 Niskin bottles was deployed and discrete samples were collected for one shallow cast (0-500 dbar) and one deep cast (0-bottom). Standard levels were chosen for the deep cast (bottom, 2000 dbar, 1500 dbar, 1250 dbar, 1000 dbar, 750 dbar, 500 dbar, salinity maximum, 200 dbar, chlorophyll maximum, 10 dbar). The shallow cast was composed of six standard levels (500 dbar, 200 dbar, 150 dbar, 50 dbar, 10 dbar, 5 dbar) and five levels dedicated to the sampling of the deep chlorophyll maximum. This sampling strategy has been reduced to a single cast (0-1000 dbar) in case of rough sea conditions, or extended with another cast (0-1000 dbar) for calibration purposes. The number of casts and samples are summarized in Table 1, with a total of 60 pigment samples, 148 oxygen samples, and 154 nutrient samples.

The cruise was prepared in coordination with the Euro-Argo infrastructure so that series of Argo and BGC-Argo floats were provided by different European institutes (BSH Germany, OGS Italy, LOV France). Hereinafter, only the BGC-Argo component is considered. At the time of the cruise, there were twelve active floats; four of these floats have been recovered and ten new floats have been deployed during the cruise. The standard way consisted in deploying BGC-Argo floats at the end of every stations, as listed in Table 2. Calibration exercises have been drawn assumed that the CTD casts and the first float profiles can be considered as co-located in time and space. That is why the floats were programmed to profile everyday at noon at the beginning of their mission. The first deep profile (0-1000 m) acquired by the floats could occur the day of the station if deployed early in the morning, or the day after if deployed later, as reported in Table 2.

This protocol of deployment is effective if a working clearance in the area of the station was obtained in order to perform CTD casts. Unfortunately, this was not the case in the eastern Levantine basin where the definitions of maritime exclusive economic zones are still vague. In consequence, one BGC-Argo float has been deployed without any reference CTD cast in the eastern Levantine (out of the list reported in Table 2). Two other floats were deployed in the same area some days after in the same conditions, however the calibration exercise was performed in the station west Levantine by clamping the floats on the frame of the CTD-Carousel and acquiring a profile (identified as BCN in Table 2) in concomitancy with the reference CTD profile and discrete samples.

The aims of this paper are to describe the collected dataset. The sensing means and the underlying processing tools for data acquired from the ship and from BGC-Argo floats are detailed in the next section. The description and the way to access to the quality controlled dataset are provided. Finally, a discussion is drawn about the various methodological strategies to update the BGC-Argo network in the Mediterranean Sea and to provide in-situ calibration of the sensors.

2 Methods for sensing, processing and quality control

The method employed for measurement (sensor technology, analytical protocol), the method used to process the collected data, and the operated quality control on the final dataset is then presented per parameter (or family of parameters).

2.1 Ocean currents

5 2.1.1 Presentation of the different measurements

Ocean currents were measured with acoustic Doppler current profilers (ADCP), along the ship track and at every station using two dedicated instruments.

The vessel has been equipped since January 2015 with an Ocean Surveyor 75 kHz interfaced with a GPS and a gyro-compass. For the cruise, the ship ADCP (hereafter SADCP) was programmed in broadband single-ping profile mode, over 70 bins of 8 m and a blanking distance of 8 m. The maximum range obtained was 500 m, it was reduced to 250 m in the ultra-oligotrophic waters of the Oriental basin.

The CTD-Carousel was equipped with a lowered ADCP (hereafter LADCP) system. It was composed of two RDI's Workhorse Monitors 300 kHz, one uplooker was clamped in the upper part of the frame that removed one over 12 Niskin bottles, and one downlooker clamped in the lower frame. The two sensors were synchronized by a command WM15. The system was supplied by an external battery box installed in the lower frame. The LADCP was programmed in narrowband mode with a sampling rate of 1 Hz and 20 bins of 8 m and a blanking distance null, earth coordinate with tilts 3 beam solution and bin mapping.

2.1.2 Data processing

Data flow from SADCP was archived on board and pre-processed using the manufacturer's software VMDAS, providing 2-minutes averaged velocity profiles. At least once per day, the data collection was uploaded and processed using the software Cascade V6.2 (Le Bot et al., 2011): ocean currents were generated by correcting raw velocity profiles from the ship navigation and attitude. **Bottom detections were masked** using Gebco 1' bathymetry, corrections of ocean tides were not applied. Two datasets were **assembled**: one set with a time resolution of 2 minutes for ocean current profiles acquired during stations, one set with a spatial resolution of 1 km for ocean current profiles acquired during transits.

Data flow from LADCP system was processed using the software LDEO IX (Thurnherr, 2014). The architecture of this software allows to replay processing chain with different parameterisations: depth computation whether from bottom track or using the concomitant CTD profile, the threshold of percentage of good values, the assimilation of SADCP data and the weight of this constraint, whether time resolution (1-second nominal) or vertical resolution (5 m bins), adjustment of the variation of magnetic declination.

LADCP data were processed with different levels of complexity. Right after each cast, a first screening of measurements was performed in order to validate the functioning of the system and assess the percentage of good values. When CTD profile **were** available, a first ocean current profile was computed with refined depth constraint. In a final step, the misfit with a mean SADCP profile during station was attempted to be minimized by iteratively processing LADCP data with this new constraint.

2.1.3 Data quality control

An in-situ calibration of SADCPC sensor has been achieved during the cruise. An L-shape of 10nm length was crossed back and forth by the ship in calm sea state and moderate speed over a shallow area of the eastern coast of Crete (see Figure 1). Bottom track was acquired all the time which allowed to compare ocean currents during the way in and the way back, supposedly steady over the 2h duration of the exercise. The two transects were significantly different in amplitude and azimuth. Corrections on misalignment angle (1.1 degree), amplitude factor (1.004) and pitch thresholds (1 and 1.5 degree) for the SADCPC have been proposed in order to reduce the misfits between transects. [Note that this calibration exercise would have been prevented in case of using CODAS software that proposes the option to compute the misalignment angle of the SADCPC.](#) Quality controlled data set of ocean currents along ship track have been post-processed thanks to these corrections.

This post-processed SADCPC dataset was also performed during stations in order to assess and improve the quality the LADCPC profiles. As reported in Table 3, all the profiles unless at casts 3 and cast 10 are characterized by low velocity errors and acceptable misfits with SADCPC profiles. [The median value of these uncertainties over the 12 acceptable casts using 1-second resolution profiles \(approximately 800 ensembles\) was evaluated to \$-0.94 \pm 3.1 \text{ cm.s}^{-1}\$ in module and \$5.4 \pm 38\$ degree in azimuth without the SADCPC constraint. Under SADCPC constraint the median value reaches to \$0.17 \pm 1.1 \text{ cm.s}^{-1}\$ in module and \$-0.02 \pm 23\$ degree in azimuth.](#) It is shown that the SADCPC constraint does not significantly improves the ocean current estimate in module, but does in azimuth. The quality controlled data set of ocean currents at stations have been processed with SADCPC constraint and binned at 5 m resolution.

2.2 Seawater temperature and practical salinity

2.2.1 Presentation of the different measurements

Temperature and practical salinity properties of seawater were continuously measured at surface along ship track by the underway system of the vessel, and at depth by the underwater unit or by the BGC-Argo floats during the seven stations. A SeaCat thermosalinograph (SBE21, serial number 3146), hereafter TSG, was mounted in the underway system of the vessel. This instrument is composed of a conductivity cell and a local temperature probe in order to derive practical salinity. A remote temperature probe (SBE38, serial number 0528) interfaced with the TSG was located at the inlet of the underway flow to minimize thermal contamination. A factory calibration of the TSG system was performed within the year preceding the cruise (29 July 2014). The acquisition started on 13 May 0:00 UTC, it was halted during port calls.

The underwater unit was equipped with a CTD (SBE911+, serial number 0329) that interfaced an internal pressure sensor, an external temperature probe (SBE3plus, serial number 2473) and an external conductivity cell (SBE4C, serial number 1313). A factory calibration of the two sensors was performed within the month preceding the cruise (16 April 2015). The GO-SHIP guidelines (Hood et al., 2010) were followed for the preparation, the maintenance, and the deployment procedure of this instrument package.

The BGC-Argo floats were equipped with factory calibrated CTD modules (SBE41CPs). These modules are designed as for mooring sensors to guarantee long-term stability of temperature, conductivity and pressure measurements. The probes were plumbed in a U-shaped seawater circuit entrained with a pump and taped with anti-foulant devices.

2.2.2 Data processing

5 The TSG data flow of 15 seconds resolution was archived on board together with GPS data flow as unmodifiable hexadecimal encoded files. At least once per day, the data collection was processed to feed a single time series of 5-minutes resolution for UTC time, geolocation, temperature, practical salinity.

During stations, seawater properties were sampled at 24 Hz with the CTD unit and transmitted on board through an electro-mechanical sea cable and slip-ring equipped winch. At-sea processing of the archive was run after each CTD cast following

10 GO-SHIP guidelines (Hood et al., 2010).

Data from BGC-Argo floats were transmitted on land via satellite Iridium communication and disseminated by a dedicated server. The continuous acquisition at 0.5 Hz is performed during the ascent phase of the float, pressure, temperature and practical salinity were decimated then processed before transmission following user's specifications: in the pressure range 0-

15 pressure range of 0-10 dbar the nominal resolution is kept, in the pressure range 10-250 dbar, averages by slices of 2 dbar were computed; in the pressure range of 250-1000 dbar, averages by slices of 10 dbar were computed.

2.2.3 Data quality control

The pressure measured from the CTD unit was compared on the vessel's deck with a reading of a barometer during port calls. No significant shift was observed that would afford a post-cruise adjustment of this sensor.

20 There were not any independent samples (such as salinity bottles) or double probes in the CTD unit that would have allowed to assess the stability of the temperature and conductivity sensors. Thus, the quality of CTD data relies on frequent factory calibrations operated on the sensors: a pre-cruise bath was performed in April 2015 (less than one month before the cruise), and a post-cruise bath performed in March 2016 (less than one year after the cruise). The static drift of the temperature sensor between baths was 0.00008 °C which is one order to magnitude lower than the theoretical stability of the probe. The static conductivity ratio between baths was 1.0000321 which represents a drift of about 0.0015 mS/cm, one order of magnitude lower

25 than the theoretical stability of the probe. Given the reproducibility of the processing method, the uncertainties of measurement provided by the CTD unit should have stayed within the accuracy of the sensors, which is 0.001 °C and 0.003 mS/cm out of lowered dynamic accuracy cases (such as in sharp temperature gradients).

The data collection of temperature and practical salinity profiles at every station is thus used as reference to assess the two other sensing systems: the TSG and the BGC-Argo floats. Systematic comparisons between the profiles from the CTD unit

30 and the neighbouring data have been lead at every casts.

Considering TSG data set, the median value of temperature and practical salinity over a time window of one hour around profile date was extracted from the 5-minute resolution time series. The comparison with the surface value from profiles has

shown a spread distribution of misfits for temperature, with an average 0.009 °C, and a narrower distribution of misfits for practical salinity with an average of 0.007. Given the nominal accuracy expected by the TSG system and in absence of systematic marked shift in the comparison, no post-cruise adjustment has been performed. The uncertainty of measurement in the TSG data set should have stayed under the 0.01 °C in temperature and 0.01 in practical salinity.

5 Considering BGC-Argo floats, the comparison with CTD profiles was performed over the layer 750 dbar – 1000 dbar, [where water mass characteristics would remain stable enough to ascribe misfits as instrumental calibration shifts whether than natural variability](#). The misfits between temperature measurements and practical salinity measurement at geopotential horizons were computed and median values provided for every BGC-Argo floats. The median offsets are reported in Table 2. They amplitudes remained of 0.01°C in temperature or 0.01 in practical salinity, unless in two cases. A large temperature offset stand for WMO
10 6901769. A large practical salinity offset was reported for WMO 6901765 however deployed in exact concomitancy with the CTD profile.

2.3 Oxygen concentration

2.3.1 Presentation of the different measurements

Concentration of dissolved dioxygen (O₂) in seawater, hereafter described as oxygen, was measured with three techniques: the
15 classical iodometric Winkler method, an electrochemical oxygen sensor, optical oxygen sensors.

Oxygen concentration was measured following the Winkler method (Winkler, 1888) with potentiometric endpoint detection (Oudot et al., 1988) on discrete samples collected with Niskin bottles. For sampling, reagents preparation and analysis, the recommendations from Langdon (2010) have been carefully followed.

[Oxygen concentrations have been measured by a Seabird SBE43 \(serial number 0587\) electrochemical sensor interfaced with
20 the CTD unit. This sensor was plumbed in the pumped circuit following the GO-SHIP guidelines \(Hood et al., 2010\).](#)

[Oxygen optical measurements \(also called optode measurements\) were collected by two types of sensors.](#) One Rinko III dissolved oxygen sensor from JFE Advanced Co. Japan (serial number 171) was interfaced with the CTD unit using the analog output voltage. Aandeeraa 4330 optodes were mounted on every BGC-Argo floats.

2.3.2 Data processing

25 The titration volumes were converted to oxygen concentrations in $\mu\text{mol.kg}^{-1}$ by following the calculation procedure proposed in Langdon (2010). The precision of the Winkler measurements was estimated by reproducibility tests based on 5 or 6 replicates for samples withdrawn from same Niskin bottles. The standard deviation on the replicate measurements was lower than 0.4 $\mu\text{mol.kg}^{-1}$.

The sensor signal of the SBE43 was aligned to temperature and pressure scans considering a unique plumbing configuration
30 for cruise, by an advance of 3s. The raw signal was then converted to an oxygen concentration with 13 calibration coefficients. The method is based on the Owens and Millard (1985) algorithm that has been slightly adapted by Seabird in the data

processing software using a hysteresis correction (Sea Bird Scientific, 2014). A new set of calibration coefficients for this sensor has been determined after the cruise, it has been used to post-process the whole dataset. Only three coefficients (the oxygen signal slope, the voltage at zero oxygen signal, the pressure correction factor) among the 13 determined by the pre-cruise factory calibration of the sensor were adjusted with the following procedure. The oxygen concentrations measured by Winkler were matched with the signal measured by the sensor at the closing of the Niskin bottles. The three values were fitted by minimizing the sum of the square of the difference between Winkler oxygen and oxygen derived from sensor signal. Outliers were discarded when the residuals exceeded 2.8 standard deviation of the residuals until no more outliers remain.

The Rinko optode provided continuous voltage output at 24 Hz, which has been directly converted to an oxygen concentration with the Matlab code developed by the manufacturer. The original calibration coefficients have been used. To process the results, the temperature measured from the CTD unit was preferred to the built-in temperature of the sensor.

The Aanderaa optodes 4330 output signal is a C1 raw phase (phase from the blue light excitation), a C2 raw phase (phase from the red light excitation), and the optode temperature. The calculation of oxygen concentrations from the optode signal follows the recommendations of Thierry et al. (2016). The calibrated phase estimated from the C1 and C2 raw phases is converted in oxygen concentration by the Stern-Volmer equation proposed by Uchida et al. (2008) using seven calibration coefficients (the so-called Stern-Volmer-Uchida coefficients). The oxygen concentration is then corrected from salinity and pressure effects. The pressure compensation is estimated following Bittig et al. (2015) with a step of phase adjustment. Finally, concentrations are expressed in $\mu\text{mol.kg}^{-1}$ by using the potential density derived from the CTD measurements of BGC-Argo floats.

2.3.3 Data quality Control

Winkler measurements on discrete samples collected during upcasts were considered as the reference oxygen value because they rely on a reference material (KIO_3 standard) given with a precision on replicate measurements lower than $0.4 \mu\text{mol.kg}^{-1}$. The reference Winkler measurements were used to adjust the calibration coefficients of the CTD oxygen sensor (SBE43), as described below. The corrected oxygen profiles during downcasts from the SBE43 at stations were considered as the reference profile for optode measurements from BGC-Argo floats. This quality control was based on the downcasts profiles at 1 dbar resolution collected whether by the electrochemical sensor SBE43 or the optode RINKO.

Residuals with Winkler measurements were expressed as the difference on an isobaric horizon between the sensor oxygen and the Winkler oxygen. A sensor error was estimated as the root mean square error on the residuals. Results are reported in Figure 2, where the residuals over the entire cruise are plotted as a function of time and depth. Residuals appear higher and more variable in the upper part of the water column, most probably due to enhanced oxygen gradients and changes on isobaric horizons between downcasts and upcasts. For electrochemical measurements, no significant offset or drift were observed; the sensor error over the entire cruise is $2.4 \mu\text{mol.kg}^{-1}$. For RINKO optode measurements, the sensor error over the entire cruise was $6.0 \mu\text{mol.kg}^{-1}$ and a systematic offset of $4.8 \mu\text{mol.kg}^{-1}$ was observed. Moreover, a significant increase of the residuals with depth ($0.0022 \mu\text{mol.kg}^{-1}.\text{dbar}^{-1}$) was observed below 200 dbar. Thus, the SBE43 data have been used rather than the RINKO data in the final record.

Considering BGC-Argo floats, it has been reported that a systematic shift in the optode calibration coefficients can occur during storage and shipment of the sensors (Bittig et al., 2012). In order to compensate this potential shift, float oxygen measurements were corrected based on a reference profile as in Takeshita et al. (2013). A slope and offset value were determined for every deployed optodes in order to adjust a posteriori the calculated oxygen values from the raw signals. The adjustment of optode values were performed using a linear model, below the first 50 dbar to avoid strong variability in the surface layer, and above the last 50 dbar to get rid of possible hooks at the bottom of profiles. The results, reported on Table 2, show a consistent correlation between the two sensors and offsets ranging from $-14 \mu\text{mol.kg}^{-1}$ to $11 \mu\text{mol.kg}^{-1}$.

2.4 Chlorophyll-a concentration

2.4.1 Presentation of the different measurements

The chlorophyll-a concentration ([Chl-a], sum of chlorophyll-a, divinyl chlorophyll-a and chlorophyllide-a) in seawater was measured with two methods: the high performance liquid chromatography (HPLC), and the fluorescence.

The HPLC method is used to estimate the [Chl-a] in discrete seawater samples collected from the TSG system or withdrawn from Niskin bottles. For this, 2.27 L of the seawater samples were filtered onto glass fibre filters (GF/F Whatman 25 mm), and all filters were stored in liquid nitrogen then at -80°C to further analysis in laboratory. The chlorophyll-a and other accessory phytoplankton pigments were then extracted from the filters in 100% methanol, disrupted by sonification and clarified by filtration (GF/F Whatman $0.7\mu\text{m}$) after 2 hours. Extracts were injected (within 24 hours after beginning of the extraction) on a reversed phase C8 column and 24 pigments were separated, identified and quantified according to the HPLC analytical protocol described by Ras et al. (2008).

Fluorometers provide continuous detection of chlorophyll-a. Three kinds of sensors were used during the cruise: Chelsea Aqua Tracka III fluorometer (serial number 088193) interfaced with CTD unit, ECO WetLabs fluorometers that equipped every BGC-Argo floats, and a Turner fluorometer (serial number 6241) plumbed in the TSG system of the vessel. The sensing mean is based on the fluorescence concept: irradiated by blue light, the chlorophyll-a absorbs and re-emits in the red part, and the re-emitted signal (i.e. the fluorescence) is considered proportional to the [Chl-a] (Lorenzen, 1966). However, to retrieve the exact [Chl-a] through the raw fluorescence signal, a calibration of the signal is necessary.

Note that fluorescence is affected by non-photochemical quenching, the mechanism employed by phytoplankton to protect from effects of high light intensity. As a result, amplitude of signal is reduced for an identical [Chl-a] when the measurement is performed under sun light exposure in the sea surface layer.

2.4.2 Data processing

The [Chl-a] is derived from raw fluorescence signal by a linear model using two calibration coefficients: an offset that corresponds to the value of the signal in the absence of [Chl-a], a scaling factor to align the signal on the exact in situ [Chl-a]. These calibration coefficients are generally provided by the manufacturer, but an adjustment using in-situ measurements of

[Chl-a] is recommended. The calibration method was based on the alignment of the fluorescence signal to exact in-situ discrete measurements of [Chl-a] provided by the HPLC method. For this, a least square linear regression was used with simultaneous measurements of [Chl-a] from fluorescence at the time, location and depth of collected seawater samples analysed by HPLC. The statistics associated to the linear regression were used as a quality control of the calibration.

5 Fluorometer derived [Chl-a] profiles at CTD casts were processed as follows. As a pre-processing step, the raw fluorescence measurements were corrected from possible non-photochemical quenching following the procedure of Xing et al. (2012). The linear regression was done with 61 simultaneous measurements of [Chl-a] determined by HPLC and the fluorometer. The resulting coefficients were an offset of 0.168 mg.m^{-3} and a slope of 4.016 with a coefficient of determination equal to 0.96. An alternative estimation of the offset has been performed by computing the median value of raw fluorescence profiles in the last 10 50 m of every profile. Indeed, when the water column is stratified (it was always the case here), the availability of light is not enough to allow the presence of active phytoplankton cells, thus the fluorescence signal should be null. This estimation considering all the fluorescence profiles provides an offset of $0.160 \pm 0.004 \text{ mg.m}^{-3}$.

As for CTD casts, the raw fluorescence measurements from BGC-Argo floats were corrected from possible non-photochemical quenching, and offsets were determined as median values of raw fluorescence in the last 50 m of the profiles. The estimated 15 offset values are reported in Table 2. Once offsets were adjusted, the linear regressions were performed with seven or eight simultaneous measurements of [Chl-a] obtained by HPLC at the float deployment. The estimated slopes are reported in Table 2. In average from all the calibration conducted, slopes range from 0.49 to 0.67 with an average value of 0.58; offsets range from -0.02 to 0.04 mg.m^{-3} with an average value of 0.02 mg.m^{-3} .

Considering fluorometer derived [Chl-a] along ship-track, a post-cruise estimation of the calibration coefficients for the Turner 20 Fluorometer has been achieved. The linear regression was done with 9 discrete seawater samples expressively collected at night (between 19 pm to 5 am) to avoid the non-photochemical quenching. The obtained calibration coefficients were an offset of 0.059 mg.m^{-3} and a slope of 4.831 with a coefficient of determination equal to 0.70. The raw fluorescence measurements were included in the TSG data flow of 15 seconds resolution. Its processing followed the same steps as for ship-track temperature and salinity to provide average time series by 5 minute bins.

25 2.4.3 Data quality control

In the Table 4, the list of quantified pigments and their limits of detections (calculated in ng per injection and as the concentrations corresponding to a signal-noise ratio of 3) are provided. Different quality control steps were applied during HPLC analysis, data processing and on the final dataset. During HPLC analysis, parameters such as the stability of the baseline, the injection precision and the pressure were monitored regularly in order to detect potential anomalies in the analytical process. 30 During data processing, chromatographic parameters were checked, including critical pair resolution, baseline noise, and peak width or retention time precision. Spectral data for the different peaks were verified and used for identification purposes and peak purity assessment. The final pigment database underwent a visual verification step for each pigment of every vertical

profiles and quality flags were assigned for each value. The visual check confirms that the identification and quantification of all the samples did not present any issues, such as coelution problems or baseline noise thus leading to potential uncertainties. Considering fluorescence measurements collected on CTD casts, the high coefficient of determination ($r^2=0.96$) for the linear model denotes a very good regression with HPLC data. The pair of calibration coefficients were applied in the post-processing of fluorescence data at every casts.

Considering fluorescence measurements collected by BGC-Argo floats, a good alignment with in-situ data was reached with coefficients of determination higher than 0.75 (see Table 2). Moreover, the homogeneity of slopes among the series of new sensors (thus recently factory calibrated) gives an insight on the gain (between 1.8 and 2) to be applied afterwards on fluorescence data (Roesler et al., 2017).

Considering fluorescence measurements collected on the TSG system, its range along the ship track appears very narrow (from 0.035 to 0.112 $\text{mg}\cdot\text{m}^{-3}$). In addition, a low number of simultaneous HPLC measurements is available (only 9 samples), and the coefficient of determination of the linear is lower than 0.70. Thus, the calibration effort performed is certainly not enough to be fully confident in the adjusted coefficients, although they have been applied to the TSG time series.

2.5 Nitrate concentration (and other nutrients)

2.5.1 Presentation of the different measurements

Concentration of nitrate (NO_3^-) ions in seawater were measured with two techniques: the classical colorimetric method in conjunction with nitrite, phosphate and silicate concentrations, and an optical nitrate sensor.

Nutrient samples were collected and conserved following the recommendations of Kirkwood (1992). All nutrient samples were analysed by a standard automated colorimetric system set up following Aminot and Kerouel (2007), using a Seal Analytical continuous flow AutoAnalyser III (AA3).

Optical sensor measurements were performed on BGC-Argo floats. Sensors using miniaturized ultraviolet spectrophotometers allow continuous measurements of absorbance spectra and estimations of nitrate concentrations (Johnson and Coletti, 2002). The BGC-Argo floats deployed during this cruise were equipped with SUNA-V2 (Submersible Ultraviolet Nitrate Analyser) sensors commercialized by Satlantics.

2.5.2 Data processing

Nitrate concentrations are derived from absorbance spectra using the the TCSS algorithm (Temperature Compensated Salinity Subtracted) set up by Sakamoto et al. (2009). In the Mediterranean Sea, because of specific conditions of low nitrate concentrations and high salinity (thus high bromide concentrations), optical measurements of nitrate were extremely delicate (D'Ortenzio et al., 2014). [This motivated the development of a specific algorithm adapted from TCSS that substantially improved the estimation of nitrate concentration in this area](#) (Pasqueron de Fommervault et al., 2015).

The BGC-Argo floats deployed during the cruise were transmitting the raw data of the SUNA (i.e. absorbance spectrum from 217 to 250 nm), which allowed a post-processing with the algorithm of Pasqueron de Fommervault et al. (2015). [A spike test was applied as well as a test for saturation based on the raw absorption spectrum.](#) Nitrate concentration data computed from a spectrum for which more than 25% of the channels saturate (i.e. reached the maximum value of numerical counts) were discarded. This was the case of one BGC-Argo float (WMO6901773).

2.5.3 Data quality control

The SUNA sensors also undergo offset and gain (Johnson et al., 2013) that were corrected using as reference the measurements on discrete samples. Given that surface nitrate concentrations in May and June in the Mediterranean Sea stand below the limit of detection of the sensor (Pasqueron de Fommervault et al., 2015), an offset was computed as the difference between an assumed surface concentration of zero and the mean nitrate value measured from 5 to 30m. A gain was then calculated with a match up between sensors measurements and nitrate concentration at discrete depths. Gain correction was applied only if the misfits between sensor derived and reference concentrations below 950 dbar did not exceed 10% of the deep reference value. The correction coefficients per BGC-Argo float are reported in Table 2. A slope of 1 was estimated for most of the cases, and the offsets ranged from $-2.70 \mu\text{mol.L}^{-1}$ to $3.90 \mu\text{mol.L}^{-1}$.

3 Data availability

The final data set concatenates the different collections during the cruise, which are vertical profiles and bottle samples at CTD casts, along track measurements at surface and at depth. This data set benefits for post-cruise corrections described in the previous sections. A unique convention has been used to identify bad data, absent data, or not reported data: they have been assigned to the value -999.

The quality control provided to discrete samples collection has been assigned with a quality flag. The quality code set up for WHP bottle parameters data has been used, in particular: “2: Acceptable measurement”, “5: Not reported”, “9: Sample not drawn for this measurement from this bottle”.

Data are published by SEANOE operated by SISMER within the framework of the in the information system ODATIS. Data at stations are available under doi:10.17882/51678, data along ship track are available under doi:10.17882/51691.

4 Discussion and conclusions

[With an extension of about 25 degrees in longitude, this cruise covered the central Mediterranean Sea and part of its north western and eastern basins. High resolution ADCP data \(Figure 3\) reveals some well know patterns of the surface circulation in this area \(the cyclonic gyre in the Ligurian basin, the eastward surface flow in the Levantine\) as well as ubiquitous mesoscale activity. Seven stations were chosen in this transect \(one in the Ligurian, two in the Tyrrhenian, two in the Ionian, two in the](#)

Levantine) in order to provide a large-scale record on the hydrography and biogeochemistry over the Mediterranean Sea. As shown in Figure 4 (upper left panel), there is a clear separation of water masses characteristics between the eastern and western basin, with a clear longitudinal gradient as deep waters and intermediate waters become eastwards saltier and warmer. Associated to this water mass distribution, biogeochemical traits clearly come up with important differences between basins and a relative homogeneity among basins. As shown in Figure 4 (lower left panel), the oxygen minimum of the intermediate waters is the lowest in the western stations, and deep waters are more oxygenated in basins directly influenced by winter convection (Ligurian and Ionian). The nutrient distribution shows also the eastern depletion of nitrates in deep waters, shallower nitraclines in the western basin, and the absence of nitrates in the surface layers relevant of Mediterranean oligotrophic spring regime (see Figure 4 lower right panel). These large-scale patterns are in good agreement with observations reported by previous field surveys such as BOUM in 2009 (Moutin and Prieur, 2012) or M84/3 in 2011 (Tanhua et al., 2013). Consequently, the vertical distribution of biomass is marked by a deep chlorophyll maximum; this maximum becomes higher and shallower between the eastern to western basins (see Figure 4 upper right panel). Such spatial contrasts need to be complemented by the temporal evolution of these patterns which can be achieved thanks to the BGC-Argo floats.

The dataset presented in this paper has been collected in the framework of an emerging in-situ observing system in the Mediterranean Sea. In order to characterize the seasonal cycles of phytoplankton dynamics and the biogeochemical functioning of the Mediterranean Sea, this network of twelve BGC-Argo floats collects physical and biogeochemical properties (temperature, salinity, concentration of dissolved oxygen, chlorophyll-a, nitrate) along 1000-meter depth profiles with a weekly sampling rate. In spring 2015, shipboard measurements have been acquired with the objective to provide a reference dataset for each core parameter of the in-situ observing system, verified through the inter-comparison of several in-situ sensing methods. This dataset offered the possibility to perform metrological verification of the deployed sensors, considering the misfits between the first profile of the float and the shipboard data. It is used as ancillary data to perform and distribute to the users community, delayed mode adjustments in the timeseries of these BGC-Argo floats (e.g. Schmechtig et al., 2015).

First of all, the presented dataset provides an in-situ characterization of the environmental conditions in which the exercises of verification have been conducted. Thanks to ocean currents and surface hydrography collected along the ship track, a first assessment of the circulation patterns neighbouring every stations can be drawn. Complemented with satellite observations (altimetry, images of sea surface temperature or ocean colour), the degree of stability of the water column would be diagnosed in order to rely (or not) on the co-location in space and time of the BGC-Argo float profile with reference data.

Second, the presented dataset provides material for a systematic calibration of the biogeochemical sensors active in the network. It has been shown (Table 2) the crucial role of this operation on newly deployed sensors. Concerning the oxygen optode sensors, their linear response does not seem to be affected, however offsets reaching amplitudes of $15 \mu\text{mol.kg}^{-1}$ have been reported, without any systematic bias among the set of sensors. Concerning fluorometer sensors, offsets can be corrected considering dark values at depth, however the amplitudes of the signals appeared to be overestimated by a factor between 1.5 and 2 depending on the sensor. Concerning nitrate sensors, their behaviour at deployment is similar to the optodes in terms of calibration, with a sensor-dependent offset up to $4 \mu\text{mol.L}^{-1}$ of amplitude. Overall, the biogeochemical sensors embarked on

the BGC-Argo floats have revealed inherent calibration shifts at deployment. This is in agreement with recent works on fluorometers ECO WetLabs (Roesler et al., 2017) and on oxygen optodes (Bittig et al. 2015, Bittig and Körtzinger, 2015).

The presented dataset is relevant to provide a robust evaluation of the calibration state of biogeochemical sensors, at the beginning of their mission. In addition, if an equivalent dataset is collected at the end of the mission when the BGC-Argo floats are recovered, the sensor drifts would be properly assessed from pre-mission and post-mission calibration states. This objective appears prerogative to enable an harmonisation between all the time series observed by the network.

This dataset offers a first attempt to evaluate the uncertainties that come up in the verification exercises. When measuring misfits between shipboard measurements and the first profile of the BGC-Argo floats, the natural variability of the environment can affect their complete attribution to calibration shifts. [This natural variability can be inferred by diurnal cycles for biogeochemical sensors, or to a lesser extent by mesoscale effects.](#) The expected variations would depend on the type of parameter, on the depth of inter-comparison, on the duration or on distance between profiles. Among the BGC-Argo floats deployed during the cruise, two benefited for a verification exercise in perfect concomitancy as they were clamped on the CTD-Carousel. The first results show reduced dispersion in function of depth for all the parameters. This dispersion criterion needs to be assessed more carefully with different types of match-up, in function of local environmental conditions and duration or distance with the first profile.

Preliminary conclusions stress the importance of evaluating the calibration state of the biogeochemical sensors, as well as their possible drift during several years of mission. The dataset collected during the cruise of May 2015 provided the relevant material to perform such exercises of metrological verification, and motivates its extension for the future deployments. The cruise also reveals unintentionally the possibility to perform a pre-deployment verification exercise some days before the beginning of its mission. The floats with newly verified sensors have been deployed close to recovered ones in order to continue their time series and to retrieve post-mission calibration states. If the propagation of reference between missions is satisfactory, such a protocol could be applied on conventional oceanographic cruises as it demands one station of metrological verification with floats mounted on the CTD-Carousel and changes of route for float deployment and recovery operations.

Author contribution

This dataset was collected by VT, TW, FDO, HLG and NM. TW analysed the oxygen samples, JR analysed the pigment samples, ED analysed the nutrient samples. Data processing and quality control were achieved by HLG for ocean currents and TSG, by VT for seawater hydrological properties, FDO and NM for chlorophyll-a concentration, TW, LC, HB and DL for oxygen concentration, OPF and FDO for nitrate concentration. VT, AP and EL set up BGC-Argo floats deployments and recoveries. Data management and availability was achieved by CS. VT and TW prepared the manuscript with contributions from FDO, NM, JR, LP and OPF.

Competing interests

The authors declare that they have no conflict of interest.

Acknowledgments

We would like to thank Captain Dany Deneuve and the crew of RV Tethys 2. These observational efforts were supported the project Equipex-NAOS, the Euro-Argo infrastructure, the program MerMex, and the project BAMA funded by LEFE/GMMC. We gratefully acknowledge their support.

References

- Aminot, A. and Kerouel, R.: Dosage automatique des nutriments dans les eaux marines methodes en flux continu. 188p. In *Methodes d'analyse en milieu marin*. Ifremer, ed. Editions 25 Quae ISBN 978-2-7592-0023-8, 2007.
- 10 Bittig, H. C., Fiedler, B., Steinhoff, T., and Körtzinger A.: A novel electrochemical calibration setup for oxygen sensors and its use for the stability assessment of Aanderaa optodes, *Limnol. Oceanogr.: Methods*, 10, 921–933, doi:10.4319/lom.2012.10.921, 2012.
- Bittig, H. C., Fiedler, B., Fietzek, P., and Körtzinger, A.: Pressure response of Aanderaa and Sea-Bird oxygen optodes *Journal of Atmospheric and Oceanic Technology*, 32, 2305-2317. DOI 10.1175/JTECH-D-15-0108.1, 2015.
- 15 Bittig, H.C., and Körtzinger A.: Tackling Oxygen Optode Drift: Near-Surface and In-Air Oxygen Optode Measurements on a Float Provide an Accurate in Situ Reference, *J. Atmos. Oceanic Technol.*, 32, 1536–1543. DOI 10.1175/JTECH-D-14-00162.1, 2015.
- Bosc, E., Bricaud, A., and Antoine, D.: Seasonal and interannual variability in algal biomass and primary production in the Mediterranean Sea, as derived from four years of SeaWiFS observations, *Global Biogeochemical Cycles*, 18, GB1005, 20 10.1029/2003GB002034, 2004.
- D'Ortenzio, F., Lavigne, H., Besson, F., Claustre, H., Coppola, L., Garcia, N., ... and Morin, P.: Observing mixed layer depth, nitrate and chlorophyll concentrations in the northwestern Mediterranean: A combined satellite and NO₃ profiling floats experiment, *Geophysical Research Letters*, 41(18), 6443-6451, 2014.
- D'Ortenzio, F., and D'Alcala, M.R.: On the trophic regimes of the Mediterranean Sea: a satellite analysis, *Biogeosciences*, 25 2009.
- Durrieu de Madron, X., and the MerMex group: Marine ecosystems' responses to climatic and anthropogenic forcings in the Mediterranean, *Progress in Oceanography*, 2011.
- Giorgi, F., and Lionello, P.: Climate change projections for the Mediterranean region, *Global and Planetary Change*, 2008.
- Hood et al.: The GO-SHIP repeat hydrography manual: A collection of expert reports and guidelines. IOCCP Report No.14, 30 ICPO Publication Series No. 134, Version 1, 2010.

- Johnson, K. S., and Coletti, L.J.: In situ ultraviolet spectrophotometry for high resolution and long-term monitoring of nitrate, bromide and bisulfide in the ocean, *Deep Sea Research Part I: Oceanographic Research Papers*, 49(7), 1291-1305, 2002.
- Johnson, K. S., Coletti, L.J., Jannasch, H.W., Sakamoto, C.M., Swift, D.D., and Riser, S.C.: Long-term nitrate measurements in the ocean using the In Situ Ultraviolet Spectrophotometer: sensor integration into the Apex profiling float, *Journal of Atmospheric and Oceanic Technology*, 30(8), 1854-1866, 2013.
- Kirkwood, D.S.: Stability of solutions of nutrient salts during storage, *Mar Chem* 38:151-164, 1992.
- Langdon, C.: Determination of Dissolved Oxygen in Seawater by Winkler Titration Using the Amperometric Technique In The GO-SHIP Repeat Hydrography Manual: A Collection of Expert Reports and Guidelines. Hood, E.M., C.L. Sabine, and B.M. Sloyan, eds. IOCCP Report Number 14, ICPO Publication Series Number 134. Available online at: <http://www.go-ship.org/HydroMan.html>, 2010.
- Le Bot, P., Kermabon, C., Lherminier, P., and Gaillard, F.: *Cascade V6.1: Logiciel de validation et de visualisation des mesures ADCP de coque, document utilisateur et maintenance*, Report OPS/LPO 11-01.
- Leymarie, E., et al.: Development and validation of the new ProvBioII float, *Mercator Ocean Quarterly Newsletter*, 2013.
- Lorenzen, C.J.: A method for the continuous measurement of in vivo chlorophyll concentration, *Deep Sea Res. Oceanogr. Abstr.*, 13(2), 223–227, doi:10.1016/0011-7471(66)91102-8, 1966.
- Marty, J.C., Chiaverini, J., Pizay, M.D., and Avril, B.: Seasonal and interannual dynamics of nutrients and phytoplankton pigments in the western Mediterranean Sea at the DYFAMED time-series station (1991–1999), *Deep- Sea Research II* 49, 1965–1985, 2002.
- Marty, J. C., and Chiaverini, J.: *Hydrological changes in the Ligurian Sea (NW Mediterranean, DYFAMED site) during 1995–2007 and biogeochemical consequences*, *Biogeosciences*, 7(7), 2117–2128, 2010.
- Mayot, N., D'Ortenzio, F., Ribera d'Alcalà, M., Lavigne, H., and Claustre, H.: The Mediterranean trophic regimes from ocean color satellites: a reappraisal, *Biogeoscience*, 13, 1901–1917, doi:10.5194/bg-13-1901-2016, 2016.
- Moutin, T. and Prieur, L.: *Influence of anticyclonic eddies on the Biogeochemistry from the Oligotrophic to the Ultraoligotrophic Mediterranean (BOUM cruise)*, *Biogeosciences*, 9, 3827-3855, <https://doi.org/10.5194/bg-9-3827-2012>, 2012.
- Oudot, C., Gerard, R., Morin, P., and Gningue, I.: Precise shipboard determination of dissolved-oxygen (Winkler Procedure) with a commercial system, *Limnology & Oceanography*, 33, 1, 146-150, WOS:A1988M521700015, 1988.
- Owens, W.B., and Millard Jr., R.C.: A new algorithm for CTD oxygen calibration, *J. Physical Oceanography*, 15, 621-631, 1985.
- Pasqueron de Fommervault, O., D'Ortenzio, F., Mangin, A., Serra, R., Migon, C., Claustre, H., ... and Schmechtig, C.: Seasonal variability of nutrient concentrations in the Mediterranean Sea: Contribution of Bio-Argo floats, *Journal of Geophysical Research: Oceans*, 2015.
- Ras, J., Claustre, H., and Uitz, J.: Spatial variability of phytoplankton pigment distributions in the Subtropical South Pacific Ocean: Comparison between in situ and predicted data, *Biogeosciences*, 5(2), 353–369, 2008.

- Roesler, C., Uitz, J., Claustre, H., Boss, E., Xing, X., Organelli, E., Briggs, N., Bricaud, A., Schmechtig, C., Poteau, A., D'Ortenzio, F., Ras, J., Drapeau, S., Haëntjens, N. and Barbieux, M.: Recommendations for obtaining unbiased chlorophyll estimates from in-situ chlorophyll fluorometers: A global analysis of WET Labs ECO sensors, *Limnology and Oceanography methods*, doi: 10.1002/lom3.10185, 2017.
- 5 Sakamoto, C. M., Johnson, K.S., and Coletti, L.J.: Improved algorithm for the computation of nitrate concentrations in seawater using an in situ ultraviolet spectrophotometer, *Limnol Oceanogr-Meth*, 7, 132-143, 2009.
- Siokou-Frangou, I., Christaki, U., Mazzocchi, M., Montresor, M., D'Alcalà, M.R., Vaqué, D., and Zingone, A.: Plankton in the open Mediterranean Sea: a review, *Biogeosciences*, 2010.
- Schmechtig, C., Poteau, A., Claustre, H., D'Ortenzio, F., and Boss, E.: Processing bio-Argo chlorophyll-a concentration at the DAC level. doi:10.13155/39468, 2015.
- 10 [Tanhua, T., Hainbucher, D., Schroeder, K., Cardin, V., Álvarez, M., and Civitarese, G.: The Mediterranean Sea system: a review and an introduction to the special issue, *Ocean Sci.*, 9, 789-803, <https://doi.org/10.5194/os-9-789-2013>, 2013.](https://doi.org/10.5194/os-9-789-2013)
- Thierry V., Gilbert D., Kobayashi T., Schmid C., and Kanako S.: Processing Argo oxygen data at the DAC level cookbook. <http://doi.org/10.13155/39795>, 2016.
- 15 [Sea-Bird Scientific: Application Note 64-3: SBE 43 dissolved oxygen \(DO\) sensor - hysteresis corrections. Available online at : <http://www.seabird.com/document/an64-3-sbe-43-dissolved-oxygen-do-sensor-hysteresis-corrections>, 2014.](http://www.seabird.com/document/an64-3-sbe-43-dissolved-oxygen-do-sensor-hysteresis-corrections)
- Uchida, H., Kawano, T., Kaneko, I., and Fukasawa, M.: In situ calibration of optode-based oxygen sensors, *J. Atmos. Oceanic Technol.*, 25, 2271–2281, doi:10.1175/2008JTECHO549.1, 2008.
- Winkler, L. W.: Die Bestimmung des im Wasser gelosten Sauerstoffes. *Ber. Dtsch. Chem. Ges.* 21: 2843-2853, 1888.
- 20 Xing, X., Claustre, H., Blain, S., D'Ortenzio, F., Antoine, D., Ras, J., and Guinet, C.: Quenching correction for in vivo chlorophyll fluorescence acquired by autonomous platforms: A case study with instrumented elephant seals in the Kerguelen region (Southern Ocean), *Limnology and Oceanography Methods*, 10, 483-495, 2012.

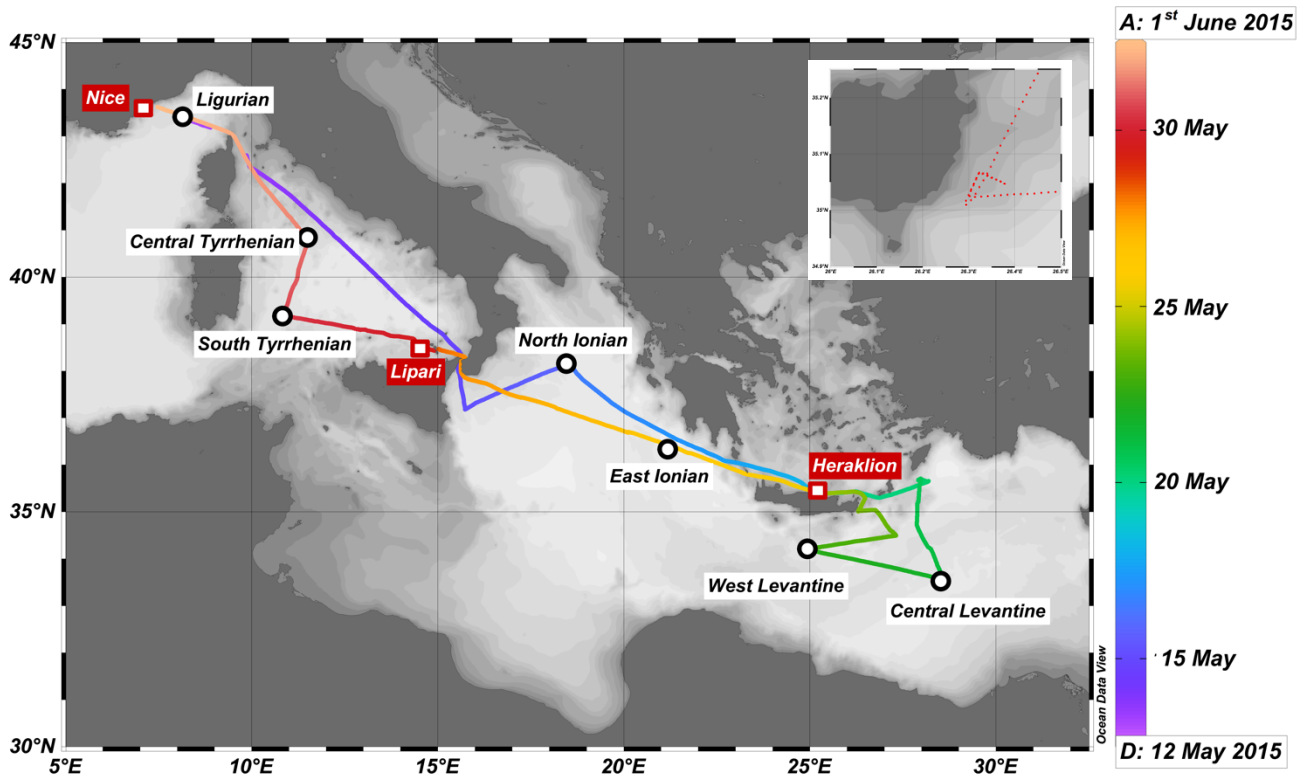


Figure 1: Cruise track plotted on a time line (colorbar). Port calls marked by red squares, stations are marked by black circles. Zoom of the L-shape track in the eastern coast of Crete.

5

STATION	CAST	DATE UTC	LATITUDE	LONGITUDE	PROFILE DEPTH (m)	BOTTOM DEPTH (m)	# SAMPLE PIGMENTS	#SAMPLE OXYGEN	# SAMPLE NUTRIENTS
LIGURIAN	1	12/5/15 20:10	43° 33.52' N	7° 27.78' E	1662	1684	5	11	11
NORTH IONIAN	2	16/05/15 03:41	38° 10.44' N	18° 30.12' E	500	3038	8	5	11
	3	16/05/15 05:35	38° 10.96' N	18° 30.16' E	2990	3038	0	11	11
CENTRAL LEVANTINE	4	21/05/15 12:21	33° 33.90' N	28° 27.99' E	500	2959*	8	11	11
	5	21/05/15 14:14	33° 33.76' N	28° 28.50' E	1240	2959*	0	11	11
WEST LEVANTINE	6	22/05/15 10:33	34° 13.89' N	24° 49.84' E	1000	2244*	7	11	11
	7	22/05/15 15:02	34° 12.61' N	24° 50.76' E	500	2886	8	11	11
	8	22/05/15 17:04	34° 12.66' N	24° 50.56' E	2871	2886	0	11	11
EAST IONIAN	9	26/05/15 12:51	36° 41.84' N	20° 07.32' E	500	3175	8	11	11
	10	26/05/15 14:44	36° 41.57' N	20° 07.21' E	3165	3175	0	11	11
SOUTH TYRRHENIAN	11	30/05/15 10:05	39° 10.43' N	10° 53.47' E	500	2812	8	11	11
	12	30/05/15 13:36	39° 11.44' N	10° 52.37' E	2803	2812	0	11	11
CENTRAL TYRRHENIAN	13	31/05/15 05:21	40° 45.22' N	11° 30.28' E	500	2466	8	11	11
	14	31/05/15 07:14	40° 45.87' N	11° 30.66' E	2456	2466	0	11	11

Table 1: Station summary. For bottom depth, values with asterisk indicate that the measurement has been obtained from the vessel's echo-sounder whether than the altimeter interfaced to the CTD unit.

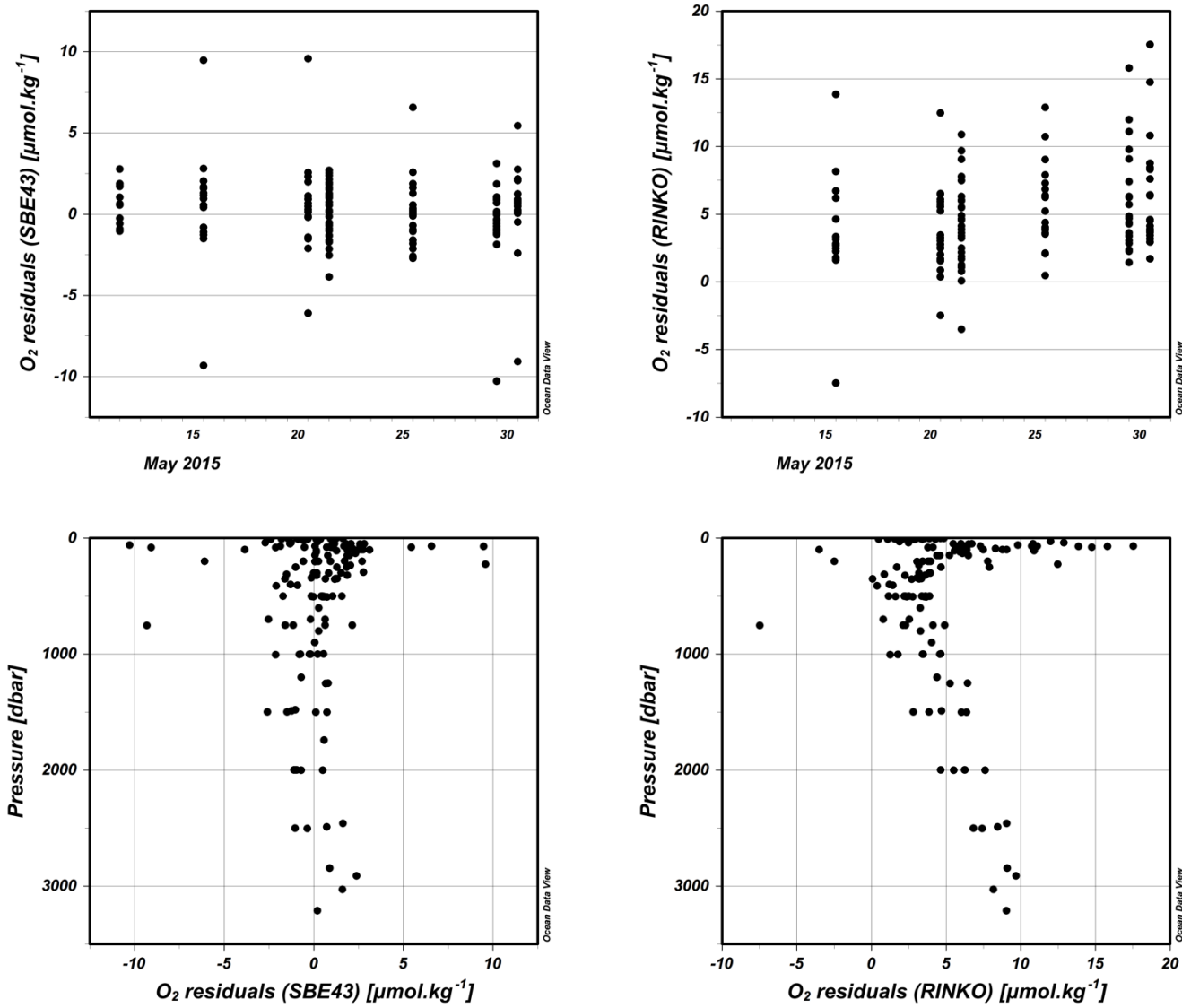
STATION	ARGO WMO	FIRST PROFILE ID	INTER-DISTANCE (km)	INTER-DURATION (h)	TEMP OFFSET (°C)	PSAL OFFEST	OPTODE SLOPE	OPTODE OFFSET ($\mu\text{mol.kg}^{-1}$)	FLUO N	FLUO R ²	FLUO OFFSET (mg.m^{-3})	FLUO SLOPE	SUNA SLOPE	SUNA OFFSET ($\mu\text{mol.L}^{-1}$)
WEST LEV.*	6901764	BCN	0	0	0.0059	0.0150	0.9796	11.56	7	0.98	0.01	0.67	1.00	3.20
WEST LEV.	6901765	000	1	19	0.0003	0.0031	1.0660	3.26	8	0.77	0.04	0.62	1.00	4.00
WEST LEV.*	6901766	BCN	0	0	0.0053	0.0081	1.0275	6.30	7	0.98	-0.02	0.65	1.11	0.80
CENTRAL TYR.	6901767	000	3	7					8	0.86	0.03	0.49	1.00	-2.80
CENTRAL TYR.	6901767	001	3	29	0.0021	-0.0009	1.1045	-3.59					1.00	-2.70
NORTH ION.	6901768	001	12	31	0.0052	0.0009	1.0235	6.66	8	0.89	0.04	0.63	1.00	2.10
SOUTH TYR.	6901769	000	2	26	0.0214	0.0050	1.1626	-14.87	8	0.82	0.03	0.58	1.00	3.90
EAST ION.	6901771	000	2	21	0.0085	0.0042	1.0658	0.51	8	0.93	0.02	0.55	1.17	0.10
CENTRAL LEV.	6901773	000	3	22	0.0067	0.0070	1.0923	-2.40	8	0.99	0.01	0.51		
AVERAGE			3	17	0.0069	0.0053	1.0652	0.93			0.02	0.59	1.04	1.08
STD			4	12	0.0064	0.0049	0.0564	8.12			0.02	0.07	0.07	2.74

* metrological verification exercise: deployed at another location than the station

Table 2: BGC-Argo float summary. For every BGC-Argo float deployed with a CTD cast of reference, the distance and duration with the first profile of the float is indicated. The results of metrological verification by parameter is reported. STD stands for standard deviation.

Cast	Depth (m)	BT distance (m)	Error velocity (cm.s ⁻¹)			LDEO final parameters	Misfits L ms S (cm.s ⁻¹)	Comments
			L without S constraint	L with S constraint	S			
1	1721	26	2.5	2.5	5.5	L+S+BT	1.8	
2	498		3.4	3.4	5.7	L+S	3.8	
3	2990	53	20.3	18.9	6.5	L+S+BT	19.2	rough sea, high tilt
4	501		3.1	2.3	6.9	L+S	3.1	5
5	1243		2.9	3.4	6.4	L+S	6.9	
6	996		2.5	2.6	5	L+S	2.0	
7	496		2.5	2.4	4.6	L+S	2.2	
8	2871	16	2.9	4.8	4.7	L+S+BT	6.1	
9	502		2.2	3.1	4.5	downlooker+S	2.6	uplooker failed, low battery
10	3165	17	20.7	50.4	5.2	downlooker+S+BT	36.0	
11	497		3	3	5.9	L+S	4.5	10
12	2805	7	5.4	4.2	6.1	L+S+BT	4.4	
13	505		2.6	2.5	5	L+S	2.5	
14	2456	12	2.8	2.8	5.3	L+S+BT	3.6	

15 **Table 3. Summary of ocean current profiles collected at the stations. Depth and bottom track (BT) distance, when available, are indicated. Error velocities were computed for three sets of profiles: LADCP (L) data only, SADCP (S) data only, L data processed under the constraint of S data. Final process parameters were chosen in function that lead to the misfits between L (with final process parameters) and S currents.**



5 Figure 2: Oxygen residuals between sensor and Winkler measurements, plotted in function of time (upper panels) and in function of depth (lower panels). The residuals for the electrochemical sensor are plotted in the left panels, the ones for the optode in the right panels.

Pigment	Variable name	Units	detection wavelength (nm)	Limit of Detection ng/inj	Limit of Detection for 2L filtered (in mg.m ⁻³)
Chlorophyll c3	CHLC3	mg.m ⁻³	450	0.015	0.0002
Chlorophyll c1+c2	CHLC2	mg.m ⁻³	450	0.018	0.0002
Sum Chlorophyllide a	CHLDA	mg.m ⁻³	667	0.016	0.0002
Peridinin	PERI	mg.m ⁻³	450	0.007	0.0001
Sum Phaeophorbid a	PHDA	mg.m ⁻³	667	0.009	0.0001
19'-Butanoyloxyfucoxanthin	BUT	mg.m ⁻³	450	0.009	0.0001
Fucoxanthin	FUCO	mg.m ⁻³	450	0.009	0.0001
Neoxanthin	NEO	mg.m ⁻³	450	0.009	0.0001
Prasincoxanthin	PRAS	mg.m ⁻³	450	0.009	0.0001
Violaxanthin	VIOLA	mg.m ⁻³	450	0.012	0.0001
19'-Hexanoyloxyfucoxanthin	HEX	mg.m ⁻³	450	0.009	0.0001
Diadinoxanthin	DIADINO	mg.m ⁻³	450	0.014	0.0002
Alloxanthin	ALLO	mg.m ⁻³	450	0.015	0.0002
Diatoxanthin	DIATO	mg.m ⁻³	450	0.015	0.0002
Zeaxanthin	ZEA	mg.m ⁻³	450	0.014	0.0002
Lutein	LUT	mg.m ⁻³	450	0.014	0.0002
Bacteriochlorophyll a	BCHLA	mg.m ⁻³	770	0.010	0.0001
Divinyl Chlorophyll b	DVCHLB	mg.m ⁻³	450	0.004	0.0001
Chlorophyll b	CHLB	mg.m ⁻³	450	0.004	0.0001
Total Chlorophyll b	TCHLB	mg.m ⁻³	450	0.004	0.0001
Divinyl Chlorophyll a	DVCHLA	mg.m ⁻³	667	0.011	0.0001
Chlorophyll-a	CHLA	mg.m ⁻³	667	0.011	0.0001
Total Chlorophyll a	TCHLA	mg.m ⁻³	667	0.011	0.0001
sum Phaeophytin a	PHYTNA	mg.m ⁻³	667	0.007	0.0001
Sum Carotenes	TCAR	mg.m ⁻³	450	0.013	0.0002

Table 4: list of parameters in the pigment dataset, the name of variable, the units, and for each pigment, the detection wavelengths and the associated limits of detection in ng per injection.

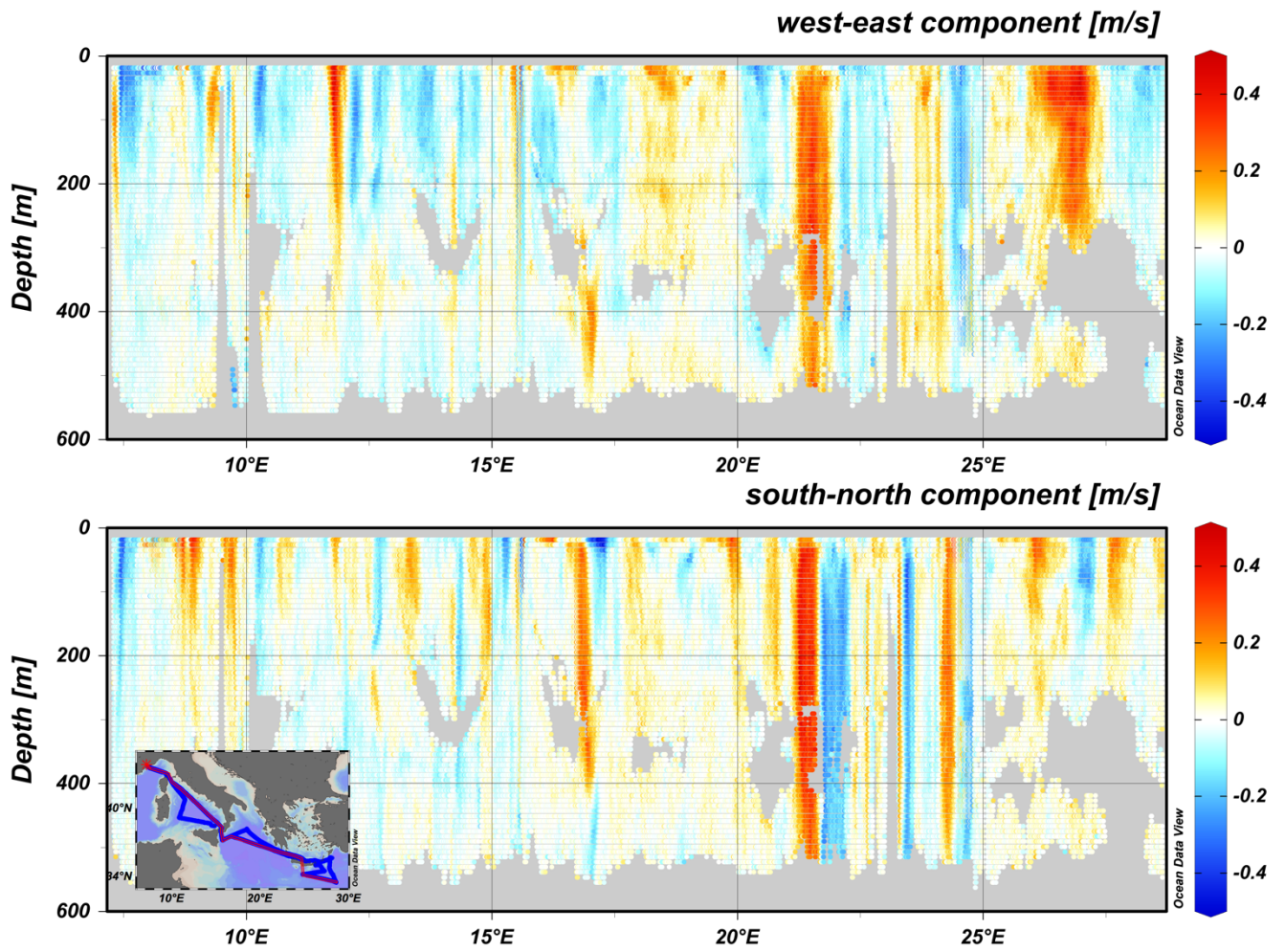


Figure 3: Velocity distribution of the upper water column along a west–east section through the Mediterranean Sea. Data are recorded by SADC. Inner panel indicates the location of the ship track and the section. Grey areas: no data are available.

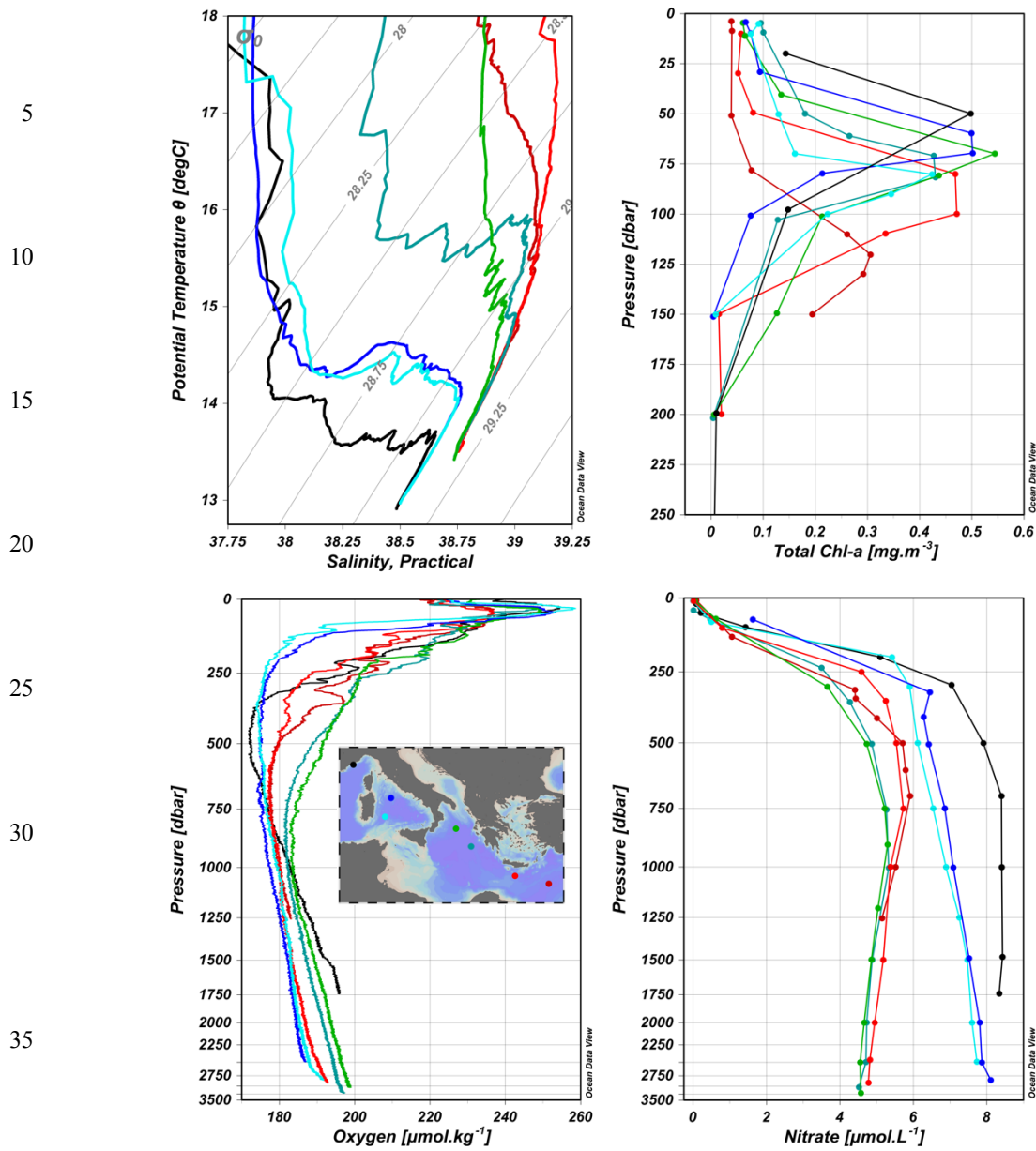


Figure 4: TS diagram determined by CTD data (upper left); total chlorophyll-a concentration profiles by HPLC method (upper right); Dissolved oxygen concentration profiles by CTD data (lower left); Nitrate concentration profiles by colorimetric method (lower right). The inner panel shows the location of CTD stations.